

Observation of carrier recombination in single Shockley stacking faults and at partial dislocations in 4H-SiC

Masashi Kato^{1,4}, Shinya Katahira¹, Yoshihito Ichikawa¹, Shunta Harada²,
Tsunenobu Kimoto³

¹*Department of Electric & Mechanical Engineering, Nagoya Institute of Technology, Nagoya 466-8555, Japan*

²*Institute of Materials and Systems for Sustainability, Nagoya University, Nagoya 464-8601, Japan*

³*Department of Electronic Science and Engineering, Kyoto University, Kyoto 615-8510, Japan*

⁴*Frontier Research institute for Materials Science, Nagoya Institute of Technology, Nagoya 466-8555, Japan*

E-mail: kato.masashi@nitech.ac.jp

Because the expansion of single Shockley stacking faults (ISSFs) is an important problem for the viability of SiC bipolar devices, there is a need to suppress it during device operation. The expansion mechanism, however, is still unclear. Therefore, the method to suppress the expansion has never been established. An important factor for the expansion could be carrier recombination in ISSFs, because the expansion has only been observed during bipolar operation or light illumination. In this study, we characterized carrier recombination by observing the photoluminescence from ISSFs and partial dislocations (PDs). The luminescence from ISSFs and PDs showed a fast decay component compared with that from the band edge. This result indicates that the carrier recombination in ISSFs and at PDs was faster than that in regions without ISSFs in 4H-SiC. In addition, because of the slower recombination at Si-core PDs compared with that in ISSFs and at C-core PDs, the velocity of ISSF expansion would be limited by the carrier recombination at Si-core PDs. The temperature dependence of the decay time implies that the recombination at the Si-core PD was enhanced on increasing the temperature.

Introduction

Silicon carbide (SiC) is widely known for its use in power semiconductor devices. To date, unipolar devices, Schottky barrier diodes, and metal–oxide–semiconductor field effect transistors that are based on SiC have been commercialized. However, the trade-off between the breakdown voltage and the on-resistance of the unipolar structure is limited by material properties. Therefore, bipolar devices are promising because of their low on-resistance and high breakdown voltage for ranges of breakdown voltage higher than ~6 kV.¹⁾

One major technical challenge for bipolar devices is suppression of bipolar degradation that is caused by the expansion of single Shockley-type stacking faults (ISSFs), which increases the forward

voltage.²⁻¹⁵⁾ Mechanisms of the expansion of 1SSFs, however, have not been fully elucidated.¹³⁻¹⁵⁾ Therefore, it is still a challenge to establish methods that suppress the expansion. The expansion is a result of the recombination enhanced dislocation glide of Si-core partial dislocations (PDs) having negative stacking fault energies of 1SSFs.^{5,16,17)} The stacking fault energy at equilibrium has been reported to have a positive value ($14.7 \pm 2.5 \text{ mJ m}^{-2}$).¹⁸⁾ Thus, 1SSFs shrink with annealing at equilibrium or under small current conduction.¹⁹⁻²¹⁾ However, 1SSFs expand under high current conduction,²⁻¹⁵⁾ light excitation,^{22,23)} or electron irradiation conditions,²⁴⁻²⁷⁾ suggesting that carrier trapping or recombination reduces the stacking fault energy. In addition, because Si-core PDs are not mobile at the usual operation temperature and stress in devices, their mobilization is induced by carrier recombination or trapping.²⁸⁾ A model for the expansion has been suggested on the basis of the concept of quasi-Fermi level or carrier trapping at Si-core PDs.²⁹⁾ Although this model treats only the steady-state condition and discusses carrier trapping at 1SSFs and Si-core PDs, the expansion is actually a dynamic phenomenon, and thus carrier recombination must be considered. Therefore, it is important to know the carrier recombination in 1SSFs and at Si-core PDs. Even though C-core PDs are immobile, the carrier recombination is of great interest.

Sridhara et al. reported carrier lifetimes in 1SSFs formed in a PiN diode by time-resolved photoluminescence (TR-PL) and observed that the carrier lifetime in 1SSFs was shorter than the bulk carrier lifetime at room temperature.⁴⁾ Chen et al. reported on electron-beam-induced current measurements for n- and p-type epilayers.^{30,31)} They found that the carrier lifetime in 1SSFs was long in an n-type epilayer and short in a p-type epilayer compared with that in the bulk. Therefore, the reported results do not agree well with each other. In addition, when the carrier lifetime in 1SSFs for an n-type epilayer is long as reported in ref. 30, the increase in the forward voltage drop by bipolar degradation is a challenge to ascribe the degradation of conductivity modulation by 1SSF expansion. Therefore, direct

measurements of the carrier recombination in 1SSFs and at Si- and C-core PDs are important to completely understand the 1SSF expansion mechanism and bipolar degradation. In this study, TR-PL measurements were carried out at luminescence wavelengths for 1SSFs and PDs in n- and p-type epilayers.

Experiments

We used two samples in this study: an n-type 4H-SiC epitaxial layer with a thickness of 100 μm and a donor concentration of $1 \times 10^{15} \text{ cm}^{-3}$,³²⁾ and a p-type 4H-SiC epitaxial layer with a thickness of 150 μm and an acceptor concentration of $6 \times 10^{14} \text{ cm}^{-3}$. A laser light with 355 nm wavelength and 1 ns pulse width was used as the excitation source for TR-PL. The densities of the injected photons were 1.4×10^{12} to $8.5 \times 10^{13} \text{ cm}^{-2}$. Luminescence from the samples was passed through a bandpass filter with transmission wavelengths of 370–410, 415–425, 661–801, and 813–1350 nm and detected by a photomultiplier. These transmission wavelengths correspond to luminescence from the band edge (~ 390 nm), 1SSFs (~ 420 nm), Si-core PDs (~ 680 and ~ 790 nm), and C-core PDs (~ 900 nm), respectively.^{4,5,9,10)} The wavelengths for PD luminescence are similar to threading edge and screw dislocations.³³⁾ The densities of the dislocations were not evaluated. The luminescence from PDs, however, is important, because PDs are present in the basal plane and thus it shows most prominent luminescence in plan view observation to the Si-face as reported in previous references.^{33,34)} The measurement temperature was controlled by hot air and a thermocouple. Measurements were performed on several regions in the samples (the spot size of the laser was 4 mm ϕ to keep signal to noise ratio for the TR-PL measurements, and the sample sizes were $\sim 1 \text{ cm}^2$). To quantify carrier recombination, we defined 1/e lifetime as the decay time constant by the time interval from the peak to 1/e of the signal.

We also performed grazing incidence synchrotron reflection X-ray topography using a monochromatic X-ray beam ($\lambda = 0.150$ nm) at BL8S2 in Aichi Synchrotron Radiation Center, Japan, to check presence of 1SSFs and PDs. The applied g vector was $11\bar{2}8$. The X-ray topography image was recorded by X-ray CMOS camera (Hamamatsu photonics C12849-101U).

Results and discussion

Figure 1 shows a X-ray topographic image for the n-type sample. The contrast from a basal plane dislocation is indicated by the arrow. Such contrasts were distributed in the entire area of the n- and p-type samples, and each basal plane dislocation has a 1SSF and S- and C-core PDs (please note that we have not performed intentional expansion procedure). Therefore, luminescence from the samples includes those from band edge and 1SSFs and PDs.

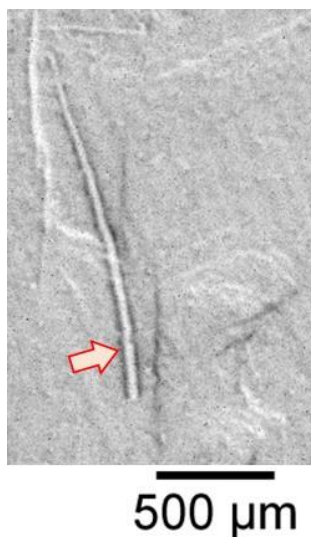


Fig. 1. X-ray topographic image for the n-type sample with g vector of $11\bar{2}8$. The arrow indicates a contrast from a basal plane dislocation.

Figure 2 shows the normalized TR-PL decay curves for luminescence from the band edge (390 nm) and 1SSFs (420 nm) obtained from two measurement regions in the n-type sample with an excitation of $8.5 \times 10^{13} \text{ cm}^{-2}$ at room temperature. Luminescence for 420 nm showed a fast component at the initial decay compared with that for 390 nm. After the initial fast decay, a slow decay was observed for one of the measurement regions (Less 1SSF). The time constants of the initial fast decay, i.e., 2.5 ns, were nearly the detection limit of our system. The initial fast decay corresponds to the carrier recombination at 1SSFs considering the wavelength. The slow decay for 420 nm from an area with low 1SSF density Less 1SSF corresponds to a luminescence tail of band edge emission.⁴⁾ From the other measurement region (More 1SSF), the slow decay was hardly observed for 420 nm, and the initial fast decay was also noticed for 390 nm. The difference in TR-PL decays between measurement regions indicates that the densities of 1SSFs were not uniform within the sample. The region with the high 1SSF density shows high intensity of luminescence band at 420 nm and low intensity of luminescence at 390 nm, because 1SSFs capture excited carriers and reduce the probability of band-to-band recombination. For the p-type sample, the luminescence at 420 nm also showed the initial fast decay. The ratio of the fast and slow decays depended on the position of the sample. Figure 3 shows the ratios of peak luminescence intensity at 390–420 nm obtained from several measurement regions. As shown in the figure, the ratio depended on the position of the sample, and 1SSF densities were not uniform in the samples.

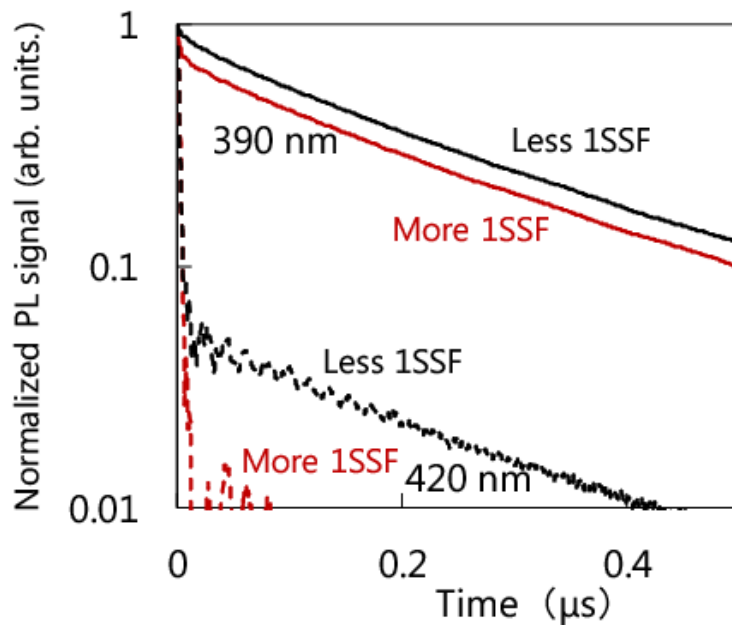


Fig. 2. Normalized TR-PL decay curves for luminescence from the band edge (390 nm) and 1SSFs (420 nm) from two measurement regions in the n-type sample with $8.5 \times 10^{13} \text{ cm}^{-2}$ excitation at room temperature.

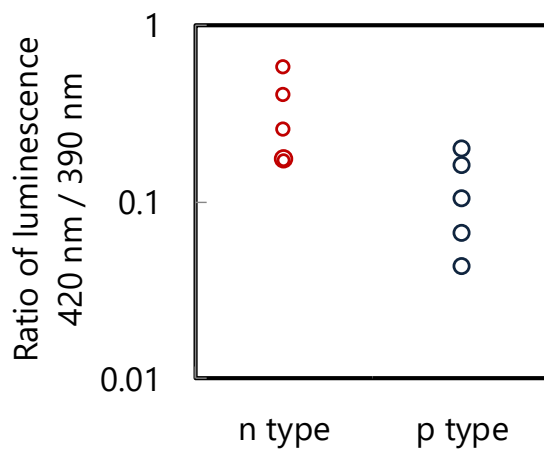


Fig. 3. Ratio of the peak luminescence intensity at 1SSFs to the band edge obtained from several measurement regions with $8.5 \times 10^{13} \text{ cm}^{-2}$ excitation at room temperature.

We then observed the excitation dependence of the TR-PL signals. Figure 4 shows the excitation dependence of TR-PL peak intensities for luminescence from the band edge, 1SSFs, Si-core PDs (680 and 790 nm) and C-core PDs (900 nm) at room temperature. The luminescence intensity for Si-core PDs was lower than that for 1SSFs, and C-core PDs had the lowest luminescence intensity. The dependence of the intensity for the band edge was superlinear at relatively high excitation, whereas that for 1SSFs was almost linear throughout the excitation. A PL signal is generally proportional to a minority carrier concentration at low injection conditions ($\propto p$ for n type). At high injection conditions, the signal becomes proportional to the product of minority and majority carrier concentrations ($\propto n \cdot p$). Therefore, the superlinear dependence of the band edge luminescence indicates that the sample became under the high injection condition on increasing the excitation. The linear dependence of 1SSF luminescence indicates that the majority carriers in 1SSFs were present at higher concentration than the excited minority carriers. Although the intensities for the PD luminescence depend on the excitation, they are smaller than the others. A quantitative discussion for the dependence, thus, is rather difficult. Excitation dependences of the peak PL signals for the p-type sample are almost the same as those for the n-type sample.

Figure 5 shows the normalized PL decay curves for the band edge luminescence from the n-type sample with three different excitations at room temperature. On increasing the excitation, the ratio of the initial fast to the subsequent slow decay components increased. The increased ratio of the fast to slow decays at the high excitation indicates the increased probability of recombination through the band edge at high injection conditions ($\propto n \cdot p$). Figure 6 shows the normalized PL decay curves for 1SSF luminescence of the n-type sample. The ratio of the initial fast to the subsequent slow components was

almost constant for different excitations. Figure 7 shows the normalized PL decay curves for PD luminescence of the n-type sample. Only $8.5 \times 10^{13} \text{ cm}^{-2}$ excitation for the C-core PD luminescence is shown because of the poor SN ratio and its small signal. The slope of the decay for Si-core PD luminescence was more gradual than that for the fast component of 1SSF luminescence, whereas the slope of the decay for C-core luminescence was almost the same as that for 1SSF luminescence. As shown in Figs. 6 and 7, the shapes of the PL decay curves for 1SSFs and PDs were independent of the excitation. This result indicates that the decays were under conditions corresponding to the low injection ones for all the excitations, which is consistent with the linear dependence of peak intensities on excitation as shown in Fig. 4. For the p-type sample, the excitation dependences of the PL decay curves were also almost the same as for the n-type sample.

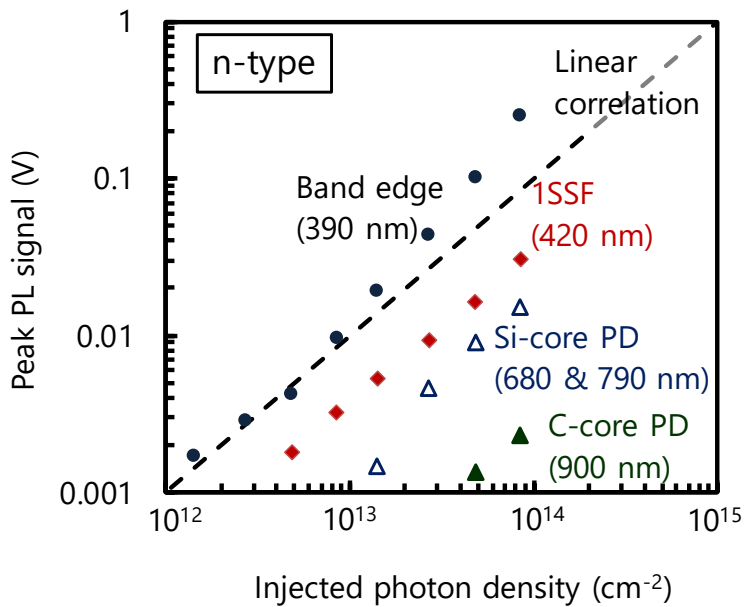


Fig. 4. Excitation dependence of the peak PL signals from the band edge, 1SSFs, and PDs for the n-type sample at room temperature.

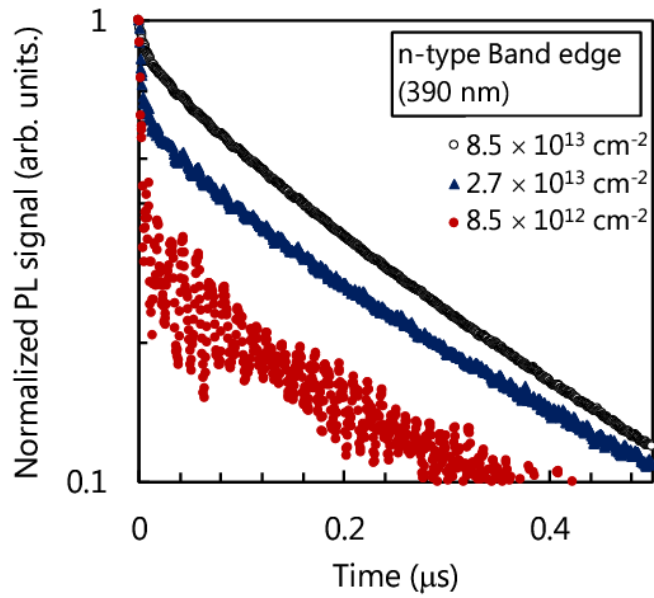


Fig. 5. TR-PL decay curves from the band edge with different excitations for the n-type sample at room temperature.

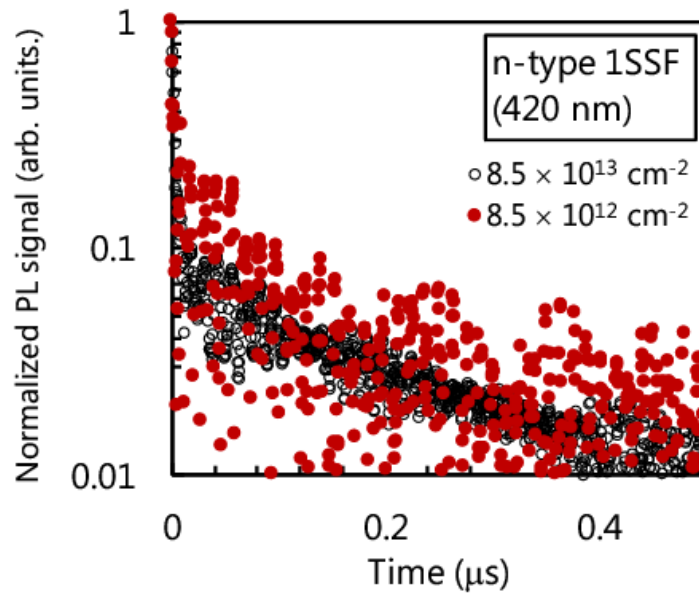


Fig. 6. TR-PL decay curves from 1SSFs with different excitations for the n-type sample at room temperature.

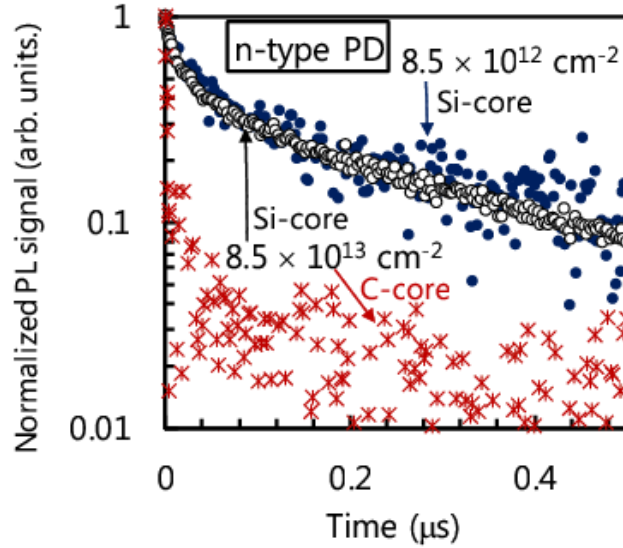


Fig. 7. TR-PL decay curves from the Si- and C-core PDs with different excitations for the n-type sample at room temperature.

We next evaluated the temperature dependence of the TR-PL decay curves. Figure 8 shows the TR-PL decay curves for 1SSF luminescence at various temperatures for the n-type sample. The slope of the decay for 1SSF luminescence was almost temperature independent and fast at all the measurement temperatures. Figure 9 shows the TR-PL decay curves for Si-core PD luminescence for the n-type sample. In contrast to 1SSF luminescence, the slope of decay for the Si-core PD luminescence showed temperature dependence. On increasing the temperature, the decay time became fast. The temperature dependence for the C-core luminescence was similar to that for the 1SSF luminescence, and the decays were very fast for all the temperatures. The temperature dependences of the TR-PL decay curves for the p-type sample were similar to those for the n-type sample.

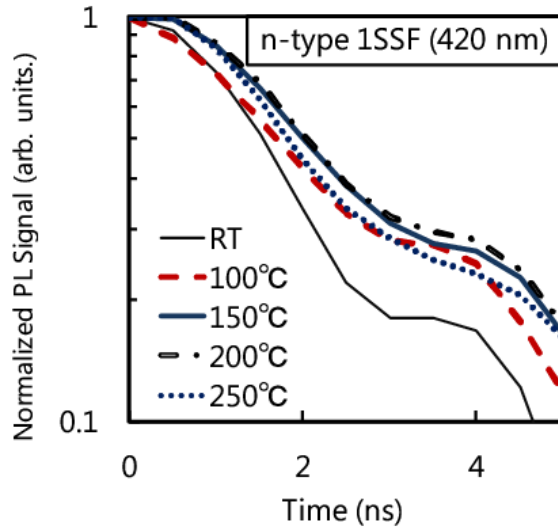


Fig. 8. Temperature dependence of TR-PL decay curves for luminescence from 1SSFs in the n-type sample excited at $8.5 \times 10^{13} \text{ cm}^{-2}$. Slight oscillation in the curves is due to noise from pulsed excitation laser.

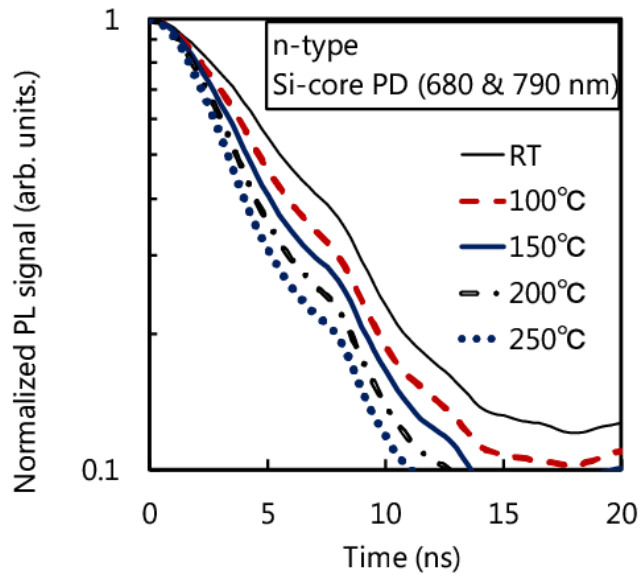


Fig. 9. Temperature dependence of TR-PL decay curves for luminescence from Si-core PDs in the n-type sample excited at $8.5 \times 10^{13} \text{ cm}^{-2}$.

We summarized the decay time for the 1SSF and PD luminescence for the n- and p-type samples by extracting the $1/e$ lifetimes as shown in Fig. 10. The $1/e$ lifetimes obtained from the decays for the 1SSF and C-core PD luminescence were less than the detection limit of our system at all the measurement temperatures for both the samples. Nevertheless, the $1/e$ lifetimes for the Si-core PD luminescence decreased with temperature for both the n- and p-type samples. Therefore, the carrier recombination at Si-core PDs, which was slower than that at 1SSFs and C-core PDs, was accelerated with temperature. The different luminescence characteristics between 1SSFs and PDs would be caused by different atomic bonding. 1SSFs have only Si-C bonds with irregular stacking sequences and act as quantum wells,³⁵⁾ while PDs have Si-Si or C-C bonds which induce energy levels in the band gap.³⁶⁾

The relatively slow carrier recombination for Si-core PDs indicates that the velocity of 1SSF expansion was limited by the carrier recombination at Si-core PDs (but not in 1SSFs). This result is consistent with the velocity enhancement of Si-core PDs by local carrier excitation as reported in ref. 23. It is the direct observation of recombination at Si-core PDs, which corresponds to an energy transfer process from excited carriers to Si-core PDs. The recombination at Si-core PDs was enhanced by increasing the temperature. The expansion velocity, thus, would also increase with the temperature. Although the recombination at C-core PDs was faster than at Si-core PDs, the luminescence intensity was very small as shown in Fig. 5. As reported in ref. 37, it has been suggested that the nonradiative recombination centers distributed around C-core PDs. Therefore, we can speculate that the C-core PD itself cannot obtain enough energy to be mobile owing to the surrounding nonradiative recombination centers. In addition, the fast carrier recombination in 1SSFs is consistent with the introduction of a high forward voltage drop in bipolar devices by expanded 1SSFs. Carriers injected in the lowly doped blocking layer immediately recombined in 1SSFs, and conductivity modulation hardly occurred for devices with expanded 1SSFs.

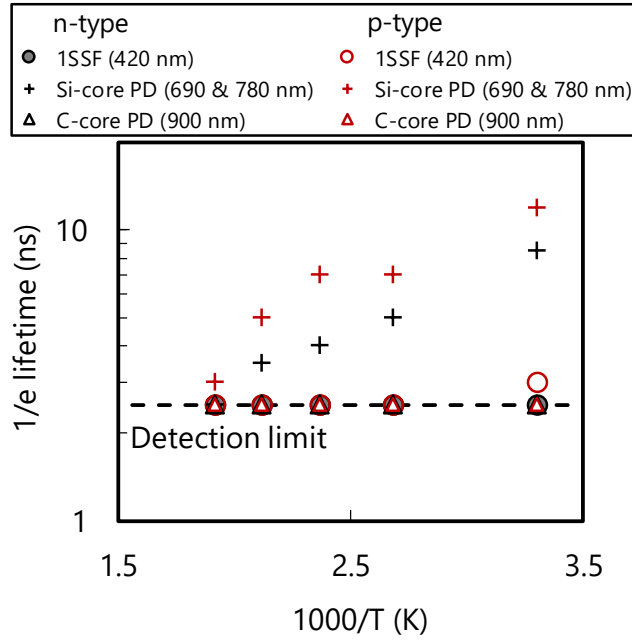


Fig. 10. Temperature dependence of 1/e lifetimes for luminescence from 1SSFs and PDs excited at $8.5 \times 10^{13} \text{ cm}^{-2}$.

Conclusions

We characterized carrier recombination at the band edge, 1SSFs, and Si- and C-core PDs in the n- and p-type 4H-SiC epilayers. The luminescence intensity depended on the position of the beam along the epilayer, indicating the nonuniform distribution of 1SSFs within the samples. By measuring at high excitation intensity, only the band edge luminescence showed signals corresponding to high injection conditions. Therefore, the majority carrier concentrations in 1SSFs and at PDs were higher than the excited minority carrier concentrations even under high excitation. The defects attract the majority carriers compared with regions without defects. Nevertheless, the carrier recombination in 1SSFs and at

PDs was faster than that at the band edge. Among the defects, Si-core PDs showed slower carrier recombination than 1SSFs and C-core PDs. This result indicates that the velocity of 1SSF expansion was limited by the carrier recombination at PDs. With increase of temperature, the carrier recombination rate at Si-core PDs increased. Considering these results, it would be possible to suppress 1SSF expansion when recombination centers are introduced around Si-core PDs.

Acknowledgments

This work was supported by JSPS KAKENHI Grant Number JP17H05331, the joint research program of the Institute of Materials and Systems for Sustainability (IMaSS), Nagoya University, and SIP (Strategic Innovation promotion Program) of the Council for Science, Technology and Innovation [Next generation power electronics/Integrated research and development of SiC for next generation power electronics] (management corporation: NEDO).

REFERENCES

- 1) M. Bakowski, IEEJ Trans. Ind. Appl. **126**, 391 (2006).
- 2) T. Kimoto and J.A. Cooper, Fundam. Silicon Carbide Technol. John Wiley & Sons Singapore (2014).
- 3) M. Skowronski and S. Ha, J. Appl. Phys. **99**, 011101 (2006).
- 4) S. G. Sridhara, F. H. C. Carlsson, J. P. Bergman, and E. Janzen, Appl. Phys. Lett. **79**, 3944 (2001).

- 5) R.E. Stahlbush, M. Fatemi, J.B. Fedison, S.D. Arthur, L.B. Rowland, and S. Wang, *J. Electron. Mater.* **31**, 370 (2002).
- 6) A. Galeckas, J. Linnros, and P. Pirouz, *Appl. Phys. Lett.* **81**, 883 (2002).
- 7) M. Skowronski, J.Q. Liu, W.M. Vetter, M. Dudley, C. Hallin, and H. Lendenmann, *J. Appl. Phys.* **92**, 4699 (2002).
- 8) J.D. Caldwell, O.J. Glembocki, R.E. Stahlbush, and K.D. Hobart, *J. Electron. Mater.* **37**, 699 (2008).
- 9) G. Feng, J. Suda, and T. Kimoto, *Appl. Phys. Lett.* **92**, 221906 (2008).
- 10) A.J. Giles, J.D. Caldwell, R.E. Stahlbush, B.A. Hull, N.A. Mahadik, O.J. Glembocki, K.D. Hobart, and K.X. Liu, *J. Electron. Mater.* **39**, 777 (2010).
- 11) K.X. Liu, R.E. Stahlbush, S.I. Maximenko, and J.D. Caldwell, *Appl. Phys. Lett.* **90**, 153503 (2007).
- 12) A. Tanaka, H. Matsuhata, N. Kawabata, D. Mori, K. Inoue, M. Ryo, T. Fujimoto, T. Tawara, M. Miyazato, M. Miyajima, K. Fukuda, A. Ohtsuki, T. Kato, H. Tsuchida, Y. Yonezawa, and T. Kimoto, *J. Appl. Phys.* **119**, 95711 (2016).
- 13) A. Galeckas, J. Linnros, and P. Pirouz, *Phys. Rev. Lett.* **96**, 025502 (2006).
- 14) K. Maeda, “Materials and Reliability Handbook for Semiconductor Optical and Electron Devices” Chap. 9, Springer Science+Business Media New York 2013.
- 15) A. Galeckas, A. Hallén, S. Majdi, J. Linnros, and P. Pirouz, *Phys. Rev. B* **74**, 233203 (2006).

- 16) Yukari Ishikawa, Masaki Sudo, Yong-Zhao Yao, Yoshihiro Sugawara, and Masashi Kato, *J. Appl. Phys.* **123**, 225101 (2018).
- 17) K. Maeda, M. Sato, A. Kubo, and S. Takeuchi, *J. Appl. Phys.* **54**, 161 (1983).
- 18) H. Idrissi, B. Pichaud, G. Regula, and M. Lancin, *J. Appl. Phys.* **101**, 113533 (2007).
- 19) M.H. Hong, A. V. Samant, and P. Pirouz, *Philos. Mag. A* **80**, 919 (2000).
- 20) J.D. Caldwell, R.E. Stahlbush, K.D. Hobart, O.J. Glebocki, and K.X. Liu, *Appl. Phys. Lett.* **90**, 143519 (2007).
- 21) T. Miyanagi, H. Tsuchida, I. Kamata, T. Nakamura, K. Nakayama, R. Ishii, and Y. Sugawara, *Appl. Phys. Lett.* **89**, 062104 (2006).
- 22) T. Tawara, S. Matsunaga, T. Fujimoto, M. Ryo, M. Miyazato, T. Miyazawa, K. Takenaka, M. Miyajima, A. Otsuki, Y. Yonezawa, T. Kato, H. Okumura, T. Kimoto, H. Tsuchida, *J. Appl. Phys.* **123**, 25707 (2018).
- 23) R. Hirano, Y. Sato, H. Tsuchida, M. Tajima, K.M. Itoh, and K. Maeda, *Appl. Phys. Express* **5**, 091302 (2012).
- 24) A. Iijima, I. Kamata, H. Tsuchida, J. Suda, and T. Kimoto, *Philos. Mag.* **97**, 2736 (2017).
- 25) Y. Yamashita, R. Nakata, T. Nishikawa, M. Hada, and Y. Hayashi, *J. Appl. Phys.* **123**, 161580, (2018).

- 26) B. Chen, J. Chen, T. Sekiguchi, T. Ohyanagi, H. Matsuhata, A. Kinoshita, H. Okumura, and F. Fabbri, *Appl. Phys. Lett.* **93**, 33514 (2008).
- 27) Y. Ohno, I. Yonenaga, K. Miyao, K. Maeda, and H. Tsuchida, *Appl. Phys. Lett.* **101**, 42102 (2012).
- 28) P. Pirouz, *Phys. Status Solidi A* **210**, 181 (2013).
- 29) T.A.G. Eberlein and R. Jones, *Appl. Phys. Lett.* **88**, 82113 (2006).
- 30) B. Chen, H. Matsuhata, T. Sekiguchi, A. Kinoshita, K. Ichinoseki, and H. Okumura, *Appl. Phys. Lett.* **100**, 132108 (2012).
- 31) B. Chen, J. Chen, Y. Yao, T. Sekiguchi, H. Matsuhata, and H. Okumura, *Appl. Phys. Lett.* **105**, 42104 (2014).
- 32) Y. Mori, M. Kato, and M. Ichimura, *J. Phys. D. Appl. Phys.* **47**, 335102 (2014).
- 33) M. Nagano, I. Kamata, and H. Tsuchida, *Jpn. J. Appl. Phys.* **52**, 04CP09 (2013).
- 34) C. Kawahara, J. Suda, and T. Kimoto, *Jpn. J. Appl. Phys.* **53**, 020304 (2014).
- 35) A. Galeckas, A. Hallén, S. Majdi, J. Linnros, and P. Pirouz, *Phys. Rev. B* **74**, 233203 (2006).
- 36) A.T. Blumenau, C.J. Fall, R. Jones, S. Oberg, T. Frauenheim, and P.R. Briddon, *Phys. Rev. B* **68**, 174101 (2003).
- 37) R. Hirano, H. Tsuchida, M. Tajima, K.M. Itoh, and K. Maeda, *Appl. Phys. Express* **6**, 011301 (2013).